Indoor Air 2008; 18: 209–224
www.blackwellpublishing.com/ina
Printed in Singapore. All rights reserved

INDOOR AIR
doi:10.1111/j.1600-0668.2008.00518.x

Particle loading rates for HVAC filters, heat exchangers, and ducts

Abstract The rate at which airborne particulate matter deposits onto heating, ventilation, and air-conditioning (HVAC) components is important from both indoor air quality (IAQ) and energy perspectives. This modeling study predicts size-resolved particle mass loading rates for residential and commercial filters, heat exchangers (i.e. coils), and supply and return ducts. A parametric analysis evaluated the impact of different outdoor particle distributions, indoor emission sources, HVAC airflows, filtration efficiencies, coils, and duct system complexities. The median predicted residential and commercial loading rates were 2.97 and 130 g/m^2 month for the filter loading rates, 0.756 and 4.35 g/m^2 month for the coil loading rates, 0.0051 and 1.00 g/month for the supply duct loading rates, and 0.262 g/month for the commercial return duct loading rates. Loading rates are more dependent on outdoor particle distributions, indoor sources, HVAC operation strategy, and filtration than other considered parameters. The results presented herein, once validated, can be used to estimate filter changing and coil cleaning schedules, energy implications of filter and coil loading, and IAQ impacts associated with deposited particles.

M. S. Waring, J. A. Siegel
The University of Texas at Austin, Department of Civil, Architectural, and Environmental Engineering, Austin, TX, USA

Key words: Particle deposition; HVAC systems; Filtration; Coil fouling; Ventilation ducts; Mass loading.

J. A. Siegel
Department of Civil, Architectural, and Environmental Engineering
The University of Texas at Austin
ECJ 5.2, 1 University Station C1752
Austin
TX 78712-1076
USA
Tel.: +1 512 471 2410
Fax: +1 512 471 3191
e-mail: jasiegel@mail.utexas.edu

Received for review 16 April 2007. Accepted for publication 30 December 2007.

Practical Implications
The results in this paper suggest important factors that lead to particle deposition on HVAC components in residential and commercial buildings. This knowledge informs the development and comparison of control strategies to limit particle deposition. The predicted mass loading rates allow for the assessment of pressure drop and indoor air quality consequences that result from particle mass loading onto HVAC system components.

Nomenclature

A_{fl}	surface area of floor (m^2)
b_f	fraction of bypass flow around the filter (dimensionless)
C_{out}	outdoor concentration of particles (mg/m^3)
d_p	particle diameter (μm)
E_c	particle mass emission rate distribution function for cooking (mg/μm h)
E_k	particle mass emission rate distribution function for indoor source, k (mg/μm h)
E_r	particle mass emission rate distribution function for resuspension (mg/μm h)
E_s	particle mass emission rate distribution function for smoking (mg/μm h)
L_{fl}	mass loading distribution of particles on floor surfaces (mg/μm m^2)
m_c	size-resolved mass deposited on the coil per volume of air (mg/μm m^3)
$M_{c,tot}$	total mass deposited on the coil per month of operation (g/month)
m_{dr}	size-resolved mass deposited on the return duct per volume of air (mg/μm m^3)
$M_{dr,tot}$	total mass deposited on the return duct per month of operation (g/month)
m_{ds}	size-resolved mass deposited on the supply duct per volume of air (mg/μm m^3)
$M_{ds,tot}$	total mass deposited on the supply duct per month of operation (g/month)
m_f	size-resolved mass deposited on the filter per volume of air (mg/μm m^3)
$M_{f,tot}$	total mass deposited on the filter per month of operation (g/month)
$n_{m,in}$	indoor particle mass distribution function (mg/μm m^3)
$n_{m,out}$	outdoor particle mass distribution function (mg/μm m^3)
$n_{N,out}$	outdoor particle number distribution function (number/μm m^3)
p	penetration of particles through cracks in the building envelope (–)
Q_i	infiltration air volumetric flow rate (m^3/h)

Q_r	recirculation air volumetric flow rate (m^3/h)
Q_v	ventilation air volumetric flow rate (m^3/h)
R	particle resuspension rate (1/h)
V	volume of the space (m^3)
β	particle deposition loss rate (1/h)
Γ	particle mass concentration ratio with and without resuspension (−)
Δt_{HVAC}	time of HVAC operation for each month (h/month)
η_c	particle deposition fraction on the coil (−)
η_{dr}	particle deposition fraction for the return ducts (−)
η_{ds}	particle deposition fraction for the supply ducts (−)
η_f	particle removal efficiency for the filter (−)
$\eta_{f,eff}$	effective particle removal efficiency of the filter, including bypass (−)
η_r	particle removal from recirculated air by HVAC system (−)
η_v	particle removal from ventilation air by HVAC system (−)
λ_i	infiltration air exchange rate (1/h)
λ_r	recirculation air exchange rate (1/h)
λ_v	ventilation air exchange rate (1/h)

Introduction

Airborne particulate matter continually deposits on components of operating heating, ventilation, and air-conditioning (HVAC) systems. Particle deposition is a strong function of particle size and researchers have characterized size-resolved particle deposition to HVAC filters (Hanley et al., 1994; Hinds, 1999), heat exchangers (Siegel, 2002; Siegel and Nazaroff, 2003), and ducts (Sippola and Nazaroff, 2003, 2004, 2005; Zhao and Wu, 2006a,b). The particle mass loading rate to an HVAC system component is the product of the particle mass concentration immediately upstream of that component, the deposition fraction onto the component, and the volumetric flow rate through the HVAC system.

Particle deposition on filters, heat exchangers (i.e. coils), and ducts can potentially generate positive and negative indoor air quality (IAQ) and energy consequences. Many particle-laden filters have higher particle removal efficiencies than when clean (Hanley et al., 1994), leading to reduced particle concentrations and improved IAQ. Also, several researchers have shown that ozone is removed by particle-laden filters. However, ozone removal can produce byproducts, such as formaldehyde, that can contribute to the degradation of actual and perceived IAQ (Bekö et al., 2006; Hyttinen et al., 2003; Zhao et al., 2007). Filters, coils, and ducts can also act as reservoirs from which biological contaminants can resuspend into the air stream (Batterman and Burge, 1995).

From an energy perspective, the pressure drop across a filter or coil increases with particle loading (ARTI, 2004; Fisk et al., 2002; Hanley et al., 1994; Siegel and Nazaroff, 2003), so the HVAC system either has a lower airflow rate or requires more fan energy to move the same amount of air, depending on the system design and type of fan control. One field study demonstrated improvements in HVAC system efficiency when coils for an office building were cleaned (Montgomery and Baker, 2006).

Because of the range of potential issues caused by particle mass accumulation on HVAC system components, knowledge of filter, coil, and duct loading rates would greatly benefit indoor environmental engineers, health scientists, industrial hygienists, HVAC system and component designers, and facilities and maintenance engineers, among others. However, we are not aware of any research that has determined loading rates for HVAC system components under typical conditions or examined the influence of building, HVAC system, and environmental parameters on loading rates. The purpose of this modeling study was to determine the monthly particle mass loading rates of residential and commercial filters, coils, and ducts. We calculated 0.001–100 μm particle size-resolved mass loading rates for typical measured and modeled parameters from the literature, grouped into the following six parameter categories: (i) Ambient distribution, (ii) Emissions indoors including resuspension, (iii) Flow and air makeup through the HVAC system, (iv) Filtration efficiency including bypass, (v) Coil properties, and (vi) Duct complexity. The results illustrate the importance of each of these parameter categories and their relative influence on the monthly loading rates.

Methodology

In this modeling study, a scenario is defined as a unique combination of parameters. The monthly loading rates (g/month) for each scenario were determined by multiplying the mass of particles that would deposit on the filter, coil, and supply and return ducts per unit volume of airflow (mg/m^3) by the total HVAC volumetric flow for a month of operation (m^3/month). Most parameters were particle size dependent and a particle diameter (d_p) range of 0.001–100 μm was considered. Residential and commercial spaces were modeled separately because of differences in values of input parameters and HVAC and ventilation system operation. Each unique parameter combination was modeled, resulting in 720 residential and 648 commercial scenarios.

Figure 1 shows the schematic that was used to account for particle fate and transport in the (a) residential and (b) commercial models. The residential model does not have ventilation air intake,

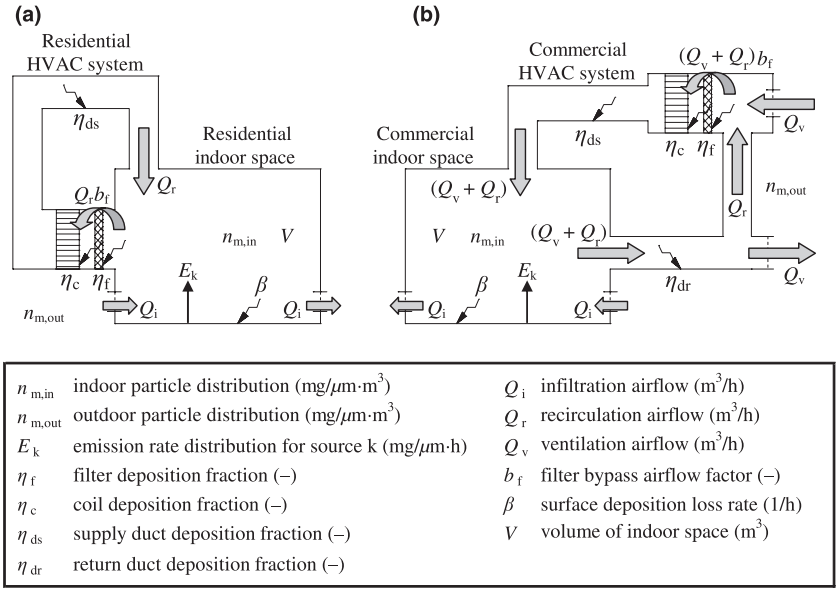

Fig. 1 Schematic for modeling of particle transport and fate in (a) residential and (b) commercial models. Block arrows represent airflows and line arrows represent particle losses or gains. Cross-hatched boxes represent HVAC filters and horizontally lined boxes represent HVAC heat exchangers (coils)

as most residential spaces get fresh air only from infiltration. In Figure 1, V is the volume of the modeled space (m^3), $n_{m,in}$ and $n_{m,out}$ are the respective indoor and outdoor particle mass distribution functions (mg/μm m^3), E_k represents the emission rate distribution functions (mg/μm h) for the various contributing indoor sources (k), Q_i, Q_v, and Q_r are the respective infiltration, ventilation, and recirculation volumetric flow rates (m^3/h), β is the size-resolved deposition loss rate for all surfaces in the building (1/h), and η_f, η_c, η_{ds}, and η_{dr} represent the size-resolved particle removal efficiencies for the filter, coil, supply ducts, and return ducts (–), respectively. The filter bypass factor, b_f (dimensionless), represents the amount of airflow that bypasses, rather than flows through, the HVAC filter.

Modeling monthly particle mass loading rates

The size-resolved mass distribution functions of particles that deposit on the filter, coil, and supply and return ducts per unit volume of airflow through the HVAC system were defined as m_f, m_c, m_{ds}, and m_{dr} (mg/μm m^3), respectively. These quantities are a function of particle diameter, d_p, and are represented by Equations 1, 2, 3, and 4, respectively. Equations 1–4 are each the product of the particle concentration immediately upstream of the relevant HVAC component multiplied by the deposition fraction to that component, weighted by the amounts of ventilation and recirculation air in the HVAC system at that point:

$$m_f = \frac{[n_{m,out}\eta_{f,eff}]\lambda_v}{\lambda_v + \lambda_r} + \frac{[n_{m,in}(1-\eta_{dr})\eta_{f,eff}]\lambda_r}{\lambda_v + \lambda_r}, \quad (1)$$

$$m_c = \frac{[n_{m,out}(1-\eta_{f,eff})\eta_c]\lambda_v}{\lambda_v + \lambda_r} + \frac{[n_{m,in}(1-\eta_{dr})(1-\eta_{f,eff})\eta_c]\lambda_r}{\lambda_v + \lambda_r}, \quad (2)$$

$$m_{ds} = \frac{[n_{m,out}(1-\eta_{f,eff})(1-\eta_c)\eta_{ds}]\lambda_v}{\lambda_v + \lambda_r} + \frac{[n_{m,in}(1-\eta_{dr})(1-\eta_{f,eff})(1-\eta_c)\eta_{ds}]\lambda_r}{\lambda_v + \lambda_r}, \quad (3)$$

$$m_{dr} = n_{m,in}\eta_{dr}, \quad (4)$$

where $\eta_{f,eff}$ is the effective removal efficiency of the filter, which includes the effect of bypass flow on the filter removal efficiency (–), and λ_v and λ_r are the ventilation and recirculation air exchange rates (1/h), respectively, when the HVAC system is active. Air exchange rates are the ratio of a particular flow rate (m^3/h) to the volume of the space (m^3).

All of these parameters, except the air exchange rates, λ_v and λ_r, are functions of particle diameter, d_p. Therefore, the integration over all relevant particle diameters (d_p = 0.001–100 μm) of Equations 1–4 multiplied by the total volumetric flow for a month of HVAC operation yields the loading rates for the filter, $M_{f,tot}$, the coil, $M_{c,tot}$, the supply ducts, $M_{ds,tot}$, and the return ducts, $M_{dr,tot}$ (g/month).

This calculation is represented generally by Equation 5:

$$M_{\mathrm{i,tot}} = V(\lambda_{\mathrm{v}} + \lambda_{\mathrm{r}})\Delta t_{\mathrm{HVAC}} \int_{d_{\mathrm{p}}} m_{\mathrm{i}}\, \mathrm{d}d_{\mathrm{p}}, \quad (5)$$

where Δt_{HVAC} is the number of hours in a month that the HVAC system is active (h/month) and the subscript, i, represents either the filter (f), coil (c), or supply or return ducts (ds or dr). Further, filter and coil loading rates were normalized by the loading areas (m^2). Loading areas were calculated as $V(\lambda_{\mathrm{v}} + \lambda_{\mathrm{r}})/v_{\mathrm{f}}$, where v_{f} is an assumed face velocity of 2 m/s, which is consistent with the face velocities at which the filter efficiencies and coil deposition fractions were determined. Duct loading was not normalized by area, given their much larger surface area as well as the fact that deposition will be more concentrated at certain locations in the duct, such as on bends.

The model employed a time-averaged indoor particle mass distribution function, $n_{\mathrm{m,in}}$ ($\mathrm{mg}/\mu\mathrm{m\ m^3}$), for indoor particle concentrations, as is shown in Equation 6:

$$n_{\mathrm{m,in}} = n_{\mathrm{m,out}} \frac{p\lambda_{\mathrm{i}} + \lambda_{\mathrm{v}}(1-\eta_{\mathrm{v}})}{\beta + \lambda_{\mathrm{i}} + \lambda_{\mathrm{v}} + \lambda_{\mathrm{r}}\eta_{\mathrm{r}}} + \sum_{\mathrm{k}} \left[\frac{E_{\mathrm{k}}/V}{\beta + \lambda_{\mathrm{i}} + \lambda_{\mathrm{v}} + \lambda_{\mathrm{r}}\eta_{\mathrm{r}}} \right], \quad (6)$$

where p is the penetration of particles through cracks in the building envelope (–) and λ_{i} is the air exchange rate as a result of infiltration (1/h). The removal of particles from the ventilation and recirculation air (–), η_{v} and η_{r}, respectively, are represented by Equations 7 and 8:

$$\eta_{\mathrm{v}} = 1 - (1-\eta_{\mathrm{f,eff}})(1-\eta_{\mathrm{c}})(1-\eta_{\mathrm{ds}}), \quad (7)$$

$$\eta_{\mathrm{r}} = 1 - (1-\eta_{\mathrm{dr}})(1-\eta_{\mathrm{f,eff}})(1-\eta_{\mathrm{c}})(1-\eta_{\mathrm{ds}}). \quad (8)$$

Equation 6 assumes a well-mixed environment and is the sum of two components: (i) particles that penetrate into the indoor environment from the outdoors and (ii) particles that are directly emitted indoors. It is important to note that Equation 6 is a time-averaged, rather than steady-state, expression. Riley et al. (2002) developed a time-averaged model to determine the indoor penetration of outdoor particles, which is similar to the first term on the right-hand side of Equation 6. Nazaroff and Klepeis (2004) developed a time averaged model to determine the increase in particle concentrations because of intermittent cigarette emissions, similar to the last term in Equation 6. Using Equation 6 requires the assumption that the removal parameters are either constant or not correlated in time with the outdoor distribution or the indoor emissions. In other words, particle loss rates are independent of the particle concentrations.

The residential model assumes that the HVAC system is either employed for all 24 h of the day (continuous flow setting) or on a duty cycle, for which there is airflow for 10 min each hour. Indoor source emissions were time-averaged (i.e. distributed) over the entire day and the residential monthly loading rates are what would occur over a month of operation at these time-averaged conditions. The commercial model assumed that the building HVAC system operates continuously for 12 h/day with indoor sources present continuously during that same period and the system is inactive for 12 h/day without indoor sources. These residential and commercial HVAC operating times (i.e. when there is airflow through the system) are reflected in the term Δt_{HVAC} in Equation 5.

All integration was performed numerically. Particle size-resolved parameters were divided into 116 different bins, with seven bins for particle diameters in the range of 0.001–0.01 μm, and between 20 and 30 bins for each of the remaining order of magnitude ranges between 0.01 and 100 μm. The parameters in Equations 1–8 were varied in a parametric analysis to explore their relative influence on the filter, coil, and supply and return duct loading rates.

Constant model parameters

The volume for the residential model was 391.9 m^3, which is the typical floor area (A_{fl}) from the US Bureau of the Census (2005) of 163.3 m^2 multiplied by an assumed ceiling height of 2.4 m. The volume of the commercial case was assumed as 1000 m^3, which was arbitrarily chosen because commercial buildings span a wide range of volumes, depending on their use. For buildings without indoor emissions, loading rates scale linearly with volume (Equations 5 and 6). For buildings with emissions, a change in volume may result in either higher or lower loading rates, depending on the strength of the emission source.

For density calculations in this model, it was assumed that particle density is 1 g/cm^3 for particles less than 2.5 μm in diameter and 2.5 g/cm^3 for particles greater than 2.5 μm in diameter. This assumption was made to account for the larger density of coarse particles, which are more likely to contain crustal material (Seinfeld and Pandis, 1998).

Using the methods and parameter values of Riley et al. (2002), the size-resolved penetration of particles through the building envelope (p) was calculated according to the theory of Liu and Nazaroff (2001). These calculated size-resolved penetration factors closely resemble the measured penetration factors reported in Long et al. (2001) for all but the very largest of particle diameters. Because of the lack of commercial penetration factors in the literature,

identical penetration factors were used for the residential and commercial cases. Similarly, both the residential and commercial models used the predicted fit of experimental values for β as summarized by Riley et al. (2002).

Ambient particle distribution

The ambient outdoor and indoor particle mass distribution functions, $n_{m,out}$ and $n_{m,in}$, respectively, both depend on the size-resolved outdoor particle number distribution, $n_{N,out}$ (number/μm m^3). This parameter was varied by using two different number distributions from Jaenicke (1993), labeled Rural and Urban in both his and our papers. These two distributions are synthesized distributions from various sources and were used in both the residential and commercial models. Each is described as a trimodal lognormal distribution, and the number, geometric mean diameters (d_{pi}), and log of the geometric standard deviation [log(σ_i)] that describe each of the three modes of these distributions are listed in Table 1 and are the same distributions used by Riley et al. (2002). The ambient outdoor particle number distribution was converted to the outdoor particle mass distribution function, $n_{m,out}$ (mg/μm m^3), by assuming the particles are spherical and multiplying the volume of the geometric mean of each size bin by the particle density. The resulting Rural integrated $PM_{2.5}$, PM_{10}, and PM_{100} concentrations are 7.3, 26.9, and 46.5 μg/m^3, respectively, and Urban integrated $PM_{2.5}$, PM_{10}, and PM_{100} concentrations are 43.1, 84.5, and 163 μg/m^3, respectively.

Emission from indoor sources and resuspension

Emission rates in the literature are presented either as particle mass or number. For emission rates reported in mass form, no conversion was necessary, but particle number emission rates were converted into mass emission rates with the same procedure as was used to convert the number distributions of outdoor origin to mass. Similar to the treatment of outdoor particle concentrations, we used the particle size-resolved emission rate distribution function (mg/μm h) in Equation 6. The residential model considered five indoor emission cases: None, Smoking, Cooking, Cooking and resuspension, and All (which is smoking, cooking, and resuspension), and the commercial model three: None, Smoking, and Heavy smoking.

Smoking (E_s). Klepeis et al. (2003) report that a smoked cigarette emits particle mass with the unimodal lognormal distribution listed in Table 1 (assuming a mean smoking time of 6.5 min). The residential model assumed either zero or 15 cigarettes were smoked indoors over an entire day, so the time-averaged daily integrated emission rates are zero or 5.36 mg/h. The commercial model assumed continuous smoking during the 12-h period with indoor sources and that there are zero, eight, or 16 smokers, so the time-averaged daily integrated emission rates are 0, 0.634, or 1.27 g/h. Eight smokers is the mean pre-ban smoker count reported in an evaluation of IAQ in hospitality venues before and after a smoking ban (Waring and Siegel, 2007), while 16 smokers is twice that amount and is meant to represent heavy smoking.

Cooking (E_c). Wallace et al. (2004) report the size-resolved, mean particle number emission rate for 33 residential cooking episodes (in Figure 4 of their paper). Based on the particle number emission rate and the reported local minima and maxima of the distribution, the emission rate was estimated as a unimodal lognormal distribution, with the characteristics listed in Table 1. With the assumed particle density of 1 g/cm^3, the mean cooking event has an integrated emission rate of 92.6 mg/h. The residential model assumes none or 90 min of cooking each day, so the time-averaged daily integrated emission rates are zero or 5.79 mg/h.

Table 1 Geometric mean diameters (d_{pi}) and log of geometric standard deviations [log(σ_i)] for particle lognormal distributions used in this modeling study

			Mode 1			Mode 2			Mode 3		
Parameter	Distribution	Units	Total	d_{pi} (μm)	log (σ_i) (–)	Total	d_{pi} (μm)	log (σ_i) (–)	Total	d_{pi} (μm)	log (σ_i) (–)
Ambient	Rural[a]	(number/cm^3)	6650	0.015	0.225	147	0.054	0.557	1990	0.084	0.266
	Urban[a]		99,300	0.013	0.245	1100	0.014	0.666	36,400	0.05	0.337
Emission	Cigarette[b]	(mg/h)	79.2	0.2	0.322						
	Cooking[c]	(number/h)	1.15×10^{14}	0.06	0.287						
	Floor loading[d,e]	(μg/cm^2)	17.3	0.7	0.165	42.5	10.2	0.282			

[a]Jaenicke (1993).
[b]Klepeis et al. (2003).
[c]Wallace et al. (2004).
[d]Thatcher and Layton (1995).
[e]The resuspension emission rate is the product of the floor loading, the floor area, and the resuspension rate (see Equation 9). Size-bin-resolved resuspension rates (1/h) are: 9.9×10^{-7} (0.3–0.5 μm), 4.4×10^{-7} (0.5–1 μm), 1.8×10^{-5} (1–5 μm), 8.3×10^{-5} (5–10 μm), 3.8×10^{-4} (10–25 μm), 3.4×10^{-5} (>25 μm).

Resuspension (E_r). Thatcher and Layton (1995) describe the mass emission rate as a result of particle resuspension, as in Equation 9:

$$E_r = L_{fl} A_{fl} R, \quad (9)$$

where L_{fl} is the mass loading of particles on the floor (mg/μm m^2), A_{fl} is the floor surface area (m^2), and R is the size-resolved resuspension rate (1/h). Emission as a result of resuspension increases linearly with particle mass accumulation on the floor. Our model assumed an integrated floor loading, L_{fl}, of 59.8 μg/cm^2, which is the weighted mean (60% hard surfaces and 40% carpet) of the adjusted first floor loading values in Thatcher and Layton (1995), assuming equal areas of tracked and untracked surfaces. The bimodal lognormal characteristics for floor loading are listed in Table 1 and were estimated as follows. First, the size-bin-resolved indoor concentration ratios for human activity vs. inactivity (in Figure 7 of their paper), labeled Γ herein (–), were set equal to the size-bin-resolved concentration ratios predicted by well-mixed, steady-state mass balances,

$$\Gamma = \frac{L_{fl} A_{fl} R + p\lambda_i V C_{out}}{p\lambda_i V C_{out}}, \quad (10)$$

where the C_{out} is the size-bin-resolved outdoor particle concentration (mg/m^3) and λ_i is the residential air exchange. Second, L_{fl} was solved for each bin, using values from their paper for variables in Equation 10, assuming their penetration value of unity. Finally, using the calculated size-bin-resolved values, 29% of the floor loading mass was attributed to the first mode and 71% to the second, and a bimodal lognormal distribution was fit. A_{fl} (m^2) in our residential model was previously stated as 163.3 m^2. Thatcher and Layton (1995) provide steady-state particle resuspension rates (R) for four people in a residence performing 'normal activities' for six particle-size bins (between 0.3 and >25 μm), which are listed under Table 1. The rates for the six bins were assigned to the geometric means of the lower and upper bounds of the bin ranges and the resuspension rates for the 116 bins in the residential model were calculated with linear interpolation. The residential model assumed either no resuspension or that 8 h of 'normal' resuspension were distributed over the entire day, so the time-averaged daily integrated emission rates are 0 or 4.31 mg/h.

Flow makeup, air exchange rates, and monthly hours of HVAC activity

The air exchange rates used are listed in Table 2. For the residential model, Duty (operation for one-sixth of the month, Δt_{HVAC} = 121.7 h/month) and Continuous (Δt_{HVAC} = 730 h/month) flow cases were considered, and the infiltration and recirculation air exchange rates are from the 'residential central air (CA)' case in Riley et al. (2002). For the commercial model, the HVAC system operated continuously for 12 h/day (Δt_{HVAC} = 365 h/month), and three air makeup cases were considered, with assumed air exchange rates based on engineering judgment. The 100% outside air (OA) case represents a building for which air recirculation is undesirable, such as with a laboratory or health care facility. The 10% OA/90% recirculated air (RA) case represents a lightly occupied commercial building that requires a small fraction of ventilation air and the 50% OA/50% RA case represents a more heavily occupied building.

Table 2 Summary of infiltration (λ_i), ventilation (λ_v), and recirculation (λ_r) exchange rates (1/h) used in this modeling study

Air exchange rate (1/h)	Residential		Commercial		
	Duty	Continuous	100% OA	10% OA/90% RA	50% OA/50% RA
λ_i	0.75	0.75	0.25	0.25	0.25
λ_v	0	0	4	0.4	2
λ_r	4	4	0	3.6	2

Filtration and bypass

Filter efficiency data were obtained from ASHRAE Standard 52.2 tests (ASHRAE, 2007), which were performed at independent testing laboratories, for clean Minimum Efficient Reporting Value (MERV) <5, 6, 11, and 15 filters. The ASHRAE Standard 52.2 procedure challenges filters with particles from 0.3 to 10 μm, so the fibrous filtration theory described by Hinds (1999) was used to extend the data into the full range used in this study, following the procedure in Riley et al. (2002). Furthermore, once the filter efficiency results were extended, they were modified to account for the impact of filter bypass, as described by Ward and Siegel (2005), for filters with no bypass and with the equivalent of 1-cm U-shaped gap around the entire filter. Identical bypass cases were considered for the residential and commercial cases. For the residential model, MERV <5, 6, and 11 filters were considered and for the commercial model, MERV 6, 11 and 15 filters were considered, with and without a bypass case for each. The effective filter removal efficiencies are shown in Figure 2a, and the curves labeled MERV 5b, 6b, 11b and 15b include the simulated filter bypass effects. This model assumed that each filter retains its clean efficiency value (i.e. the filter efficiency is constant over time), although efficiency typically improves with loading (Hanley et al., 1994).

Coil properties

Both the residential and commercial models used Dry and Wet coil deposition fractions for the particle diameter range of 0.001–100 μm, for a coil with 4.7 fins/cm (12 fins/inch). The deposition fraction for the

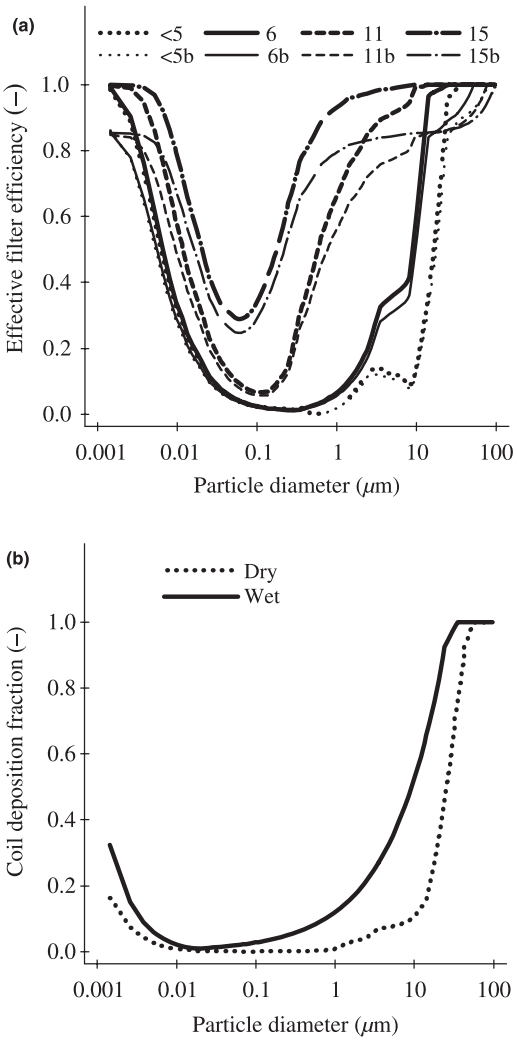

Fig. 2 (a) Effective filter efficiencies ($\eta_{f,eff}$) for MERV < 5–15 filters, including bypass cases, and (b) coil deposition fractions (η_c) for Dry and Wet coils

Dry, isothermal coil was determined using the isothermal coil deposition model in Siegel and Nazaroff (2003) to best fit their experimental data, which was for a particle diameter range of 1–20 μm. The deposition fraction for the Wet, non-isothermal coil was determined with the same procedure but with the non-isothermal model in Siegel (2002). The Dry and Wet coil deposition fractions are shown in Figure 2b. This model assumes that the coil fills the entire duct space (i.e. no coil bypass). Coils with fin pitches larger than 4.7 fins/cm would have increased coil deposition and coils with smaller fin pitches decreased deposition.

Duct complexity

The layout of ventilation ducts (i.e. length and diameter of sections, number of bends and connectors, etc.) varies widely depending on the building and the models used particle size-resolved single-pass deposition fractions for residential and commercial duct runs of three levels of complexity, taken from results in the literature. For the residential model, supply duct single-pass particle deposition fractions are from Siegel (2002), who used the duct deposition theory of Sippola and Nazaroff (2003) to calculate Simple, Typical, and Complex cases (referred to identically herein), with layout input parameters taken from ACCA (1995) and a field study of 11 houses performed in California, Nevada, and Texas (Siegel et al., 2003). Given the simplicity (or absence) of residential return ducts, they are not likely sites for deposition (Siegel et al., 2003) and are excluded. For the commercial model, the Simple, Typical, and Complex cases were the 10th, 50th, and 90th percentile cut-point single-pass particle deposition fractions modeled for return and supply ducts reported in Sippola and Nazaroff (2003), who considered 60 supply and 60 return duct runs in four university buildings.

Duct leakage was not considered, as there is inadequate information in the literature regarding particle concentrations in spaces surrounding return ducts, such as attics and crawlspaces. Return ducts are under a negative pressure and would suck particles in from these outdoor spaces, increasing loading. Leaks from positively pressurized supply ducts to outdoor spaces would decrease the particle concentrations in the indoor space, decreasing loading.

Parameter base case definitions and number of reported scenarios

The residential and commercial parameters modeled, as well as the literature sources for those values, are summarized in Table 3. A description of how each parameter will be referred to in all subsequent figures in this paper follows each one. A Rural and Urban base case for both the residential and commercial models was selected based on typical values for each parameter. Within the Rural and Urban distributions, the residential base case consisted of Cooking and resuspension as indoor emissions, a Duty flow cycle, a MERV 6 filter [the requirement for new homes in ASHRAE Standard 62.2 (ASHRAE, 2004)] without bypass, a Dry coil, and Typical residential supply ducts. Similarly, the commercial base case consisted of the None indoor source case, an airflow makeup of 10% OA/90% RA, a MERV 11 filter without bypass, a Dry coil, and Typical commercial supply and return ducts.

Each combination of the parameters was modeled, and there were 720 residential and 648 commercial scenarios. However, certain commercial parameter combinations yielded identical and redundant results. Particularly, for commercial scenarios with the Flow parameter of 100% OA (i.e. no recirculation), the filter, coil, and supply duct loading rates are independent of all parameters downstream of the respective component. These redundant scenarios were only accounted for once in our results, which led to 444 cases for

Table 3 Summary of varied parameters for residential and commercial models

Parameter	Type	Parameters (base cases in bold)	Parameter codes
Ambient[a]	Residential, commercial	**Rural, Urban**	R, U
Emission[b]	Residential	None, Smoking, Cooking, **Cooking and resuspension**, All (smoking, cooking, and resuspension)	N, S, C, Cr, A
	Commercial	**None**, Smoking, Heavy smoking	N, S, Hs
Flow[c]	Residential	**Duty**, Continuous	D, C
	Commercial	100% OA, **10% OA/90% RA**, 50%OA/50%RA	O, 19, 55
Filtration[d]	Residential	MERV: <5, **6**, 11	<5, 6, 11
	Commercial	MERV: 6, **11**, 15	6, 11, 15
	Residential, commercial	With a 1-cm bypass case for each	b
Coil[e]	Residential, commercial	**Dry**, Wet	D, W
Duct[f]	Residential, commercial	Simple, **Typical**, Complex	S, T, C

Base cases are in bold and parameter codes are used on figures of loading rate results.
[a]Jaenicke (1993).
[b]Klepeis et al. (2003), Wallace et al. (2004), Thatcher and Layton (1995) and Waring and Siegel (2007).
[c]Riley et al. (2002) and engineering judgment.
[d]Test results, Hinds (1999) and Ward and Siegel (2005).
[e]Siegel (2002) and Siegel and Nazaroff (2003).
[f]Siegel (2002) and Sippola and Nazaroff (2003).

commercial filter loading, 456 cases for coil loading, 504 cases for supply duct loading, and all 648 cases for return duct loading.

Results and discussion

The residential and commercial loading rates varied widely, depending on the input parameters. The median was used as a descriptive statistic because it is less susceptible to being skewed by extreme cases of loading and because the outdoor distributions and indoor sources are lognormally distributed. The *overall medians* for the residential and commercial loading rates were 2.97 and 130 g/m^2 month for the filter loading rates, 0.756 and 4.35 g/m^2 month for the coil loading rates, 0.0051 and 1.00 g/month for the supply duct loading rates, and 0.262 g/month for the commercial return duct loading rates. The *Rural base case* residential and commercial loading rates were 0.790 and 12.3 g/m^2 month for the filter loading rates, 0.068 and 0.045 g/m^2 month for the coil loading rates, 0.0028 and 0.034 g/month for the supply duct loading rates, and 0.0046 g/month for the commercial return duct loading rates. The *Urban base case* residential and commercial loading rates were 1.56 and 42.6 g/m^2 month for the filter loading rates, 0.143 and 0.113 g/m^2 month for the coil loading rates, 0.0055 and 0.109 g/month for the supply duct loading rates, and 0.019 g/month for the commercial return duct loading rates.

Figure 3 summarizes the residential and commercial filter, coil, and supply and return duct loading rates. Figures 3a–g are box plots of the monthly loading rates, with each box summarizing all scenarios employing the parameter listed below it, grouped by the Ambient, Emission, Flow, Filtration, Coil, and Duct parameter categories. The boxes represent the 25th to 75th percentile values and the median is the line in the middle of the box. The whiskers represent the largest values that are within 1.5 multiplied by the range represented by the box. Outliers beyond this range (i.e. an extreme case of loading) are indicated by a small circle above or below the whiskers. The thick gray line over all parameter categories is the overall median of all of the scenarios depicted in the plot, the thick black line is the Urban base case, and the thin black line is the Rural base case.

Influential parameter categories have parameter medians that vary widely from the overall median and non-influential parameter categories have parameter medians very near the overall median. The loading rates of each component are highly influenced by that component itself. However, besides these cases of self-influence, the Coil and Duct parameters have almost no influence on the loading rates. The residential filter, coil, and supply duct loading rates are significantly influenced by the Ambient and Emission source parameters, as well as the HVAC system parameters of Flow and Filtration. The loading rates for the commercial model follow similar trends to the residential model.

Using the defined base cases, parametric influence was also determined with the use of a loading rate ratio (LRR), for the filter and coil loading rates only. The ducts were excluded from all succeeding discussion because they load so little relative to the other components (duct loading is distributed over the entire duct length and filter and coil loading are normalized by area normal to the volumetric flow) and duct deposition has been studied extensively elsewhere (Sippola and Nazaroff, 2003, 2004, 2005; Zhao and Wu, 2006a,b). The LRR is equal to the *adjusted loading rate* divided by the Rural or Urban base case loading rate, and the adjusted loading rate

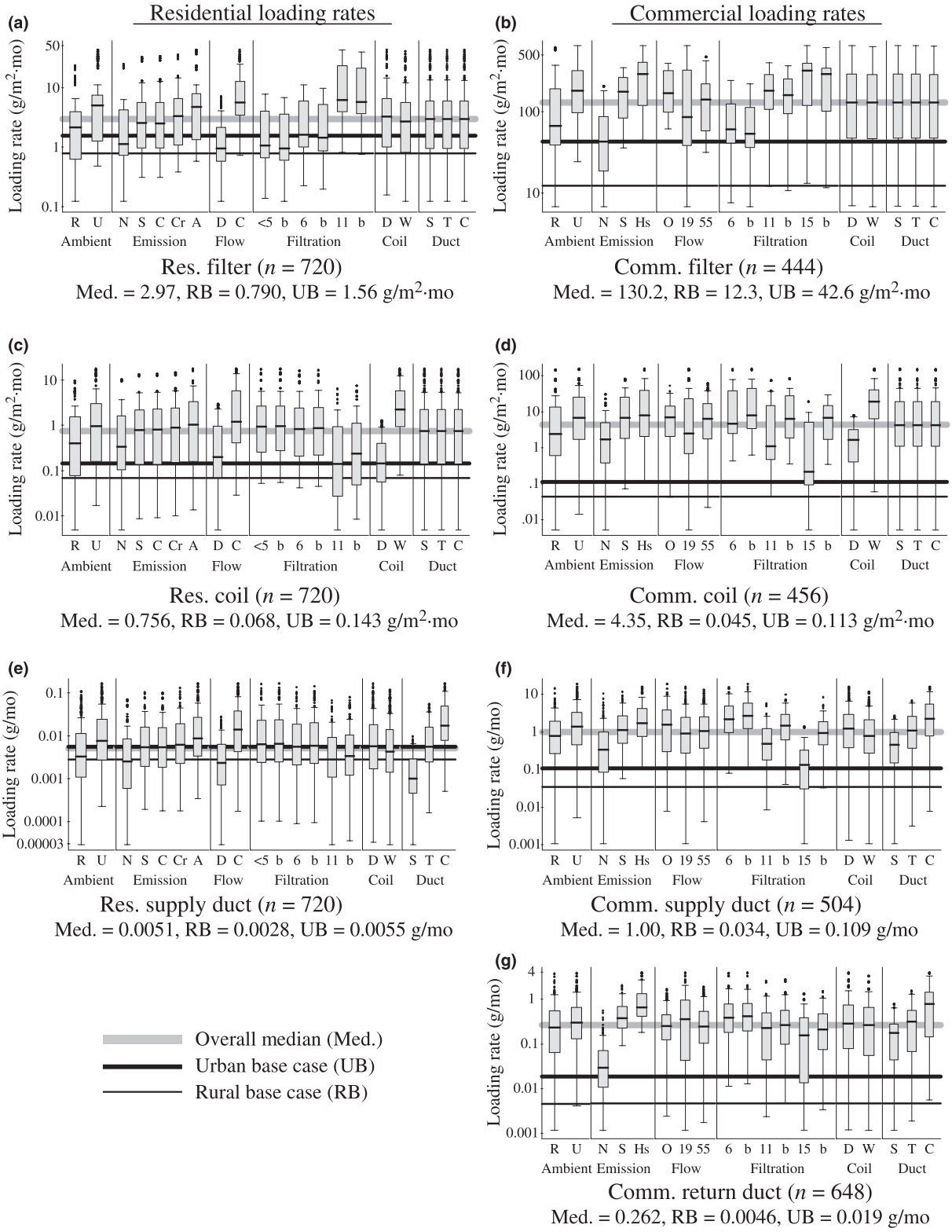

Fig. 3 Modeled (a) residential and (b) commercial filter, (c) residential and (d) commercial coil, and (e) residential and commercial (f) supply and (g) return duct loading rates, plotted on a log scale. Parameter codes on *x*-axes are listed in Table 3

is the result of holding all parameters in the base case constant except for the varied parameter. Thus, the LRR is a measure of how sensitive the loading rate is to a specific change of a given parameter, relative to the defined base case. Additionally, multiplying the base case loading rate by the appropriate LRR will yield the adjusted loading rate of interest. Table 4 lists LRRs for changing each

Table 4 Loading rate ratios (LRR = adjusted loading rate/base case loading rate) for both rural and urban base cases

				LRR			
				Filter		Coil	
Parameter	Type	Base case	Going to	Residential	Commercial	Residential	Commercial
Rural base case							
Ambient	Residential, commercial	Rural	Urban	1.98	3.46	2.10	2.53
Emission	Residential	Cooking and resuspension	None	0.36		0.62	
			All (smoking, cooking, resuspension)	1.37		1.18	
	Commercial	None	Smoking		15.56		12.70
			Heavy smoking		30.12		24.40
Flow	Residential	Duty	Continuous	6.00		6.00	
	Commercial	10%OA/90%RA	100% OA		8.77		8.23
			50% OA/50% RA		4.53		4.33
Filtration	Residential	MERV6	MERV <5	0.66		1.46	
			MERV 11	3.29		0.14	
	Commercial	MERV 11	MERV 6		0.64		10.40
			MERV 15		1.07	1.12	0.12
	Residential, commercial	No bypass	1 cm, 2 bend bypass	0.88	0.89		8.05
Coil	Residential, commercial	Dry	Wet	0.86	0.99	13.92	8.29
Duct	Residential, commercial	Typical	Simple	1.00	1.00	1.00	1.00
			Complex	1.00	1.00	1.00	0.99
Urban base case							
Ambient	Residential, commercial	Urban	Rural	0.51	0.29	0.48	0.39
Emission	Residential	Cooking and resuspension	None	0.68		0.82	
			All (smoking, cooking, resuspension)	1.19		1.09	
	Commercial	None	Smoking		5.21		5.62
			Heavy smoking		9.42		10.23
Flow	Residential	Duty	Continuous	6.00		6.00	
	Commercial	10%OA/90%RA	100% OA		8.14		7.33
			50% OA/50% RA		4.27		3.96
Filtration	Residential	MERV6	MERV <5	0.66		1.33	
			MERV 11	3.73		0.15	
	Commercial	MERV 11	MERV 6		0.65		9.65
			MERV 15		1.11		0.13
	Residential, commercial	No bypass	1 cm, 2 bend bypass	0.88	0.90	1.08	11.59
Coil	Residential, commercial	Dry	Wet	0.83	0.98	15.32	16.26
Duct	Residential, commercial	Typical	Simple	1.00	1.00	1.00	1.00
			Complex	1.00	1.00	1.00	0.99

Rural base case: residential filter = 0.790 g/m^2 month; commercial filter = 12.3 g/m^2 month; residential coil = 0.068 g/m^2 month; commercial coil = 0.045 g/m^2 month.
Urban base case: residential filter = 1.56 g/m^2 month; commercial filter = 42.6 g/m^2 month; residential coil = 0.143 g/m^2 month; commercial coil = 0.113 g/m^2 month.

parameter from the Rural and Urban base cases to other possible values.

Besides reinforcing many of the parametric trends visible in Figure 3, the use of the LRR for Rural and Urban base cases allows further insight into the effects different outdoor distributions have on residential vs. commercial filter and coil loading rates. The relative influence of indoor sources is similar within different outdoor distributions for the residential loading rates but not the commercial loading rates. Using filter loading rates as an example, going from the residential base case Emission parameter of Cooking and resuspension to the case of All indoor sources yields similar LRRs of 1.37 and 1.19 in the Rural and Urban environments, respectively. However, going from the commercial base case for the None indoor source case to Smoking yields dissimilar LRRs of 15.56 and 5.21 in the Rural and Urban environments, respectively. For the commercial model, the filter is the first point of contact for much of the air, so the indoor Emission parameter has much less of an impact in the Urban than in the Rural environment (and a corresponding lower LRR).

More nuanced trends in the loading rates can be determined by examining the results from a size-resolved perspective, also within the context of parametric influence on the loading rates. Figure 4 displays the median particle size-resolved (a) residential and (b) commercial filter loading rates, for three different parameter combinations, which are the (1) Emission parameters within each Ambient distribution and the Filtration parameters within each of the Flow cases for the (2) Rural and (3) Urban distributions. Each bar summarizes the results that use the two parameters listed below it as inputs, with the fraction of mass attributed to each size bin demarcated by a different shade within the bar. In Figure 4a-1, for example, the size-resolved bar for All indoor sources within the Rural distribution was created by summing the median

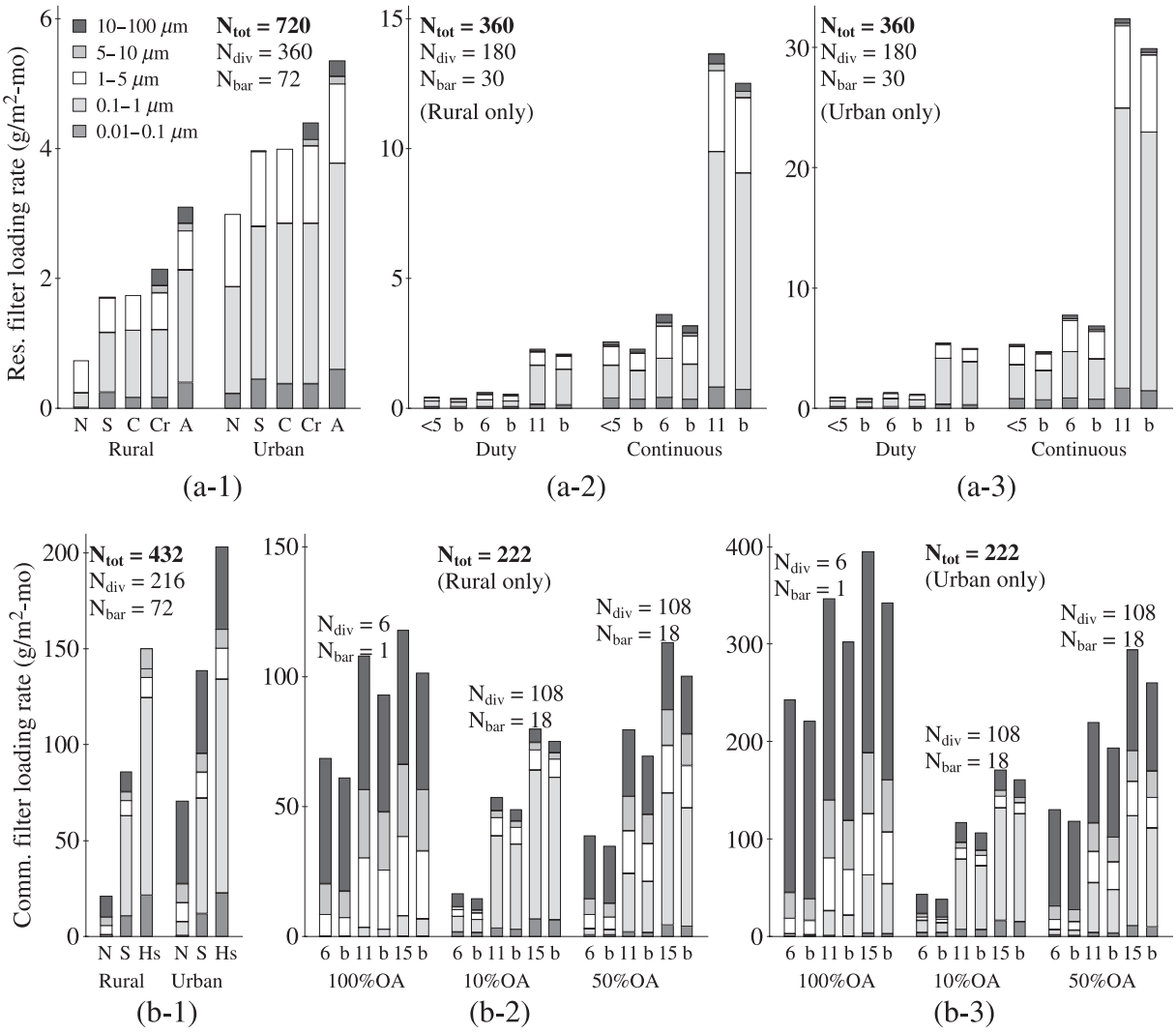

Fig. 4 Size-resolved (a) residential and (b) commercial filter loading rates (g/m^2 month), for (1) Emission parameters within each Ambient distribution, and Filtration parameters within each Flow case, for (2) Rural and (3) Urban distributions. Parameter codes on x-axes are listed in Table 3. N_{bar} represents the number of scenarios used to make each bar, N_{div} for each division of plot, and N_{tot} for total plot (differences in values between each plot reflect elimination of non-unique scenarios)

size-resolved geometric means of the loading rates for any modeled result that had All indoor sources and Rural parameters as inputs. The number of results used to make each portion of the figure varied depending on the parameter combinations: N_{bar} represents the number of scenarios used to make each bar, N_{div} for each division of the plot (e.g. the Ambient division in Figure 4a-1), and N_{tot} for the total plot.

The commercial filter loads more quickly than the residential for the following reasons. The commercial model uses higher efficiency filters. Additionally, all airflow in the residential HVAC system is recirculated and ambient air only enters the residential space because of penetration through the building envelope, which removes all particles over 5 μm in diameter. These reduced concentrations in the residential indoor air (as compared with the outdoor air) are further reduced by surface deposition (β) and infiltration air exchange loss mechanisms (λ_i), of which the commercial ventilation air passing immediately through the filter is not. Moreover, the indoor emission rates are larger for the commercial model. Finally, there is more volumetric airflow through the commercial HVAC system.

The fraction of mass loading attributed to each particle size range is dependent on whether the building is residential or commercial. For the residential filter, the mass loaded consists primarily of particles smaller than 5 μm in diameter for the Rural and Urban distributions. The only mechanism by which particles larger than 5 μm are introduced into the residential indoor air is resuspension, but resuspension as the sole origin of large particles in indoor air is not entirely supported by the literature. Wallace and Howard-Reed (2002) monitored a residence for 18 months and observed low concentrations of particles above 5 μm

in diameter when no indoor source was present. For the commercial filters, however, there is considerable mass loading because of particles greater than 5 μm in diameter, because the filter is the first particle removal point for the ventilation air stream.

Urban scenarios have larger filter loading rates than Rural scenarios. As outdoor particle concentrations increase, the relative influence of the Emission parameter on loading rates decreases. For example, residential filter loading rates for scenarios with All indoor sources are factors of 4.3 and 1.8 over scenarios with the None indoor source case, for the Rural and Urban distributions, respectively. Residential Smoking and Cooking occur for approximately the same total amount of time in a day (97.5 and 90 min, respectively) and each causes significant and similar increases in filter loading rates. For the commercial filters, Smoking and Heavy smoking substantially increase filter loading rates and these indoor sources also contribute relatively less to mass loading for scenarios with the Urban distribution (also discussed in regard to the LRR above). Note that these loading results are highly dependent on the assumptions of this model. For example, many residences use rangehood exhaust fans to reduce particle concentrations during cooking and smoking rates are highly variable.

The HVAC system parameters of Flow and Filtration have a large influence on the filter loading rates for both residential and commercial systems. For the same residential filter, the Continuous flow causes an increase over Duty flow cycles by a factor of six, because six times as much air moves through the HVAC system. In the commercial model, the HVAC flow is continuous, but the fraction of ventilation vs. recirculation air varies. Figure 4b-2 and b-3 illustrates how the mass loads differently on commercial filters for the different Flow parameters within Rural and Urban environments. For the Rural distribution, the loading rates for scenarios with 100% and 50% OA are similar in magnitude, because indoor sources have a larger relative influence in this environment. For the Urban distribution, however, the contribution to loading is dominated by the outdoor particle concentrations and the scenarios with no recirculation (100% OA) have the highest loading rates.

The filter loading rates increase with the filter efficiency, independent of any other parameter, and the efficiency influences the relative contribution of each size bin to the total mass loaded. For example, Figure 4a-2 and a-3 displays how the MERV 11 filter has a much higher fraction of mass loaded because of 0.1–1 μm diameter particles than the MERV <5 or 6 filters, because MERV 11 filters remove more of this smaller size range. The relative contributions of mass loaded because of particles larger than 1 μm are more similar because even lower efficiency filters can be effective in this size range. Moreover, bypass has a smaller relative influence on the filter loading rate for a lower than a higher efficiency filter, predominantly for scenarios for which higher concentrations of large diameter particles contact the filter (e.g. commercial scenarios with higher fractions of ventilation air). This differing influence is likely because of two reasons: (i) if the filter is poor at removing particles, it matters less if some air bypasses the filter and (ii) the higher efficiency filters are likely to have a larger pressure drop across them when compared with the lower efficiency filters. The increased pressure drop drives a larger volumetric flow rate of air through the same size bypass gap (Ward and Siegel, 2005).

Figure 5 is similar to Figure 4, but it displays the results for the residential and commercial coil loading rates. The residential and commercial coil loading rates are more comparable in magnitude than the filter loading rates, for two main reasons. The first reason is that the more efficient filters in the commercial system leads to lower loading rates because more particles are removed from the air upstream of the coil. Secondly, as shown in Figure 2b, very little deposition occurs on the coil except for particles in the largest size ranges, which again are effectively removed by the filter upstream of the coil.

The coil loading rates exhibit similar trends to the filter loading rates, with the role of filters being the main exception. Higher efficiency filters lead to lower coil loading rates and filter bypass increases coil loading rates. As with filters, bypass has a larger effect for higher efficiency filters, but for the coil loading, the effect is much more pronounced. As Figure 5b-3 illustrates, a 1-cm bypass gap around a MERV 15 filter leads to coil loading rates higher than those for a MERV 11 filter without bypass. This large dependence of the coil loading rates on filter bypass is not present in the residential model, because particles over 5 μm in diameter only exist as a result of resuspension and these larger particles affect coil loading rates the most.

It is important to revisit the limitations of this approach. The assumptions that have the largest impacts on loading rates are those related to the model input parameters. Where possible we used values from the peer-refereed literature, but we suggest caution in applying the results to a real building without sufficient knowledge of parameter values and without validation of the results presented here. Another important assumption is that the entire building was well mixed, despite the fact that some of the emission sources considered here (e.g. cooking) are likely to occur in a single zone in the building. However, given the relatively small losses because of deposition to building surfaces and in duct work, relative to filters and coils, this assumption will likely have a very small impact on the final results. Another assumption is that removal parameters are not correlated in time with the outdoor distribution or the indoor emissions, which is required

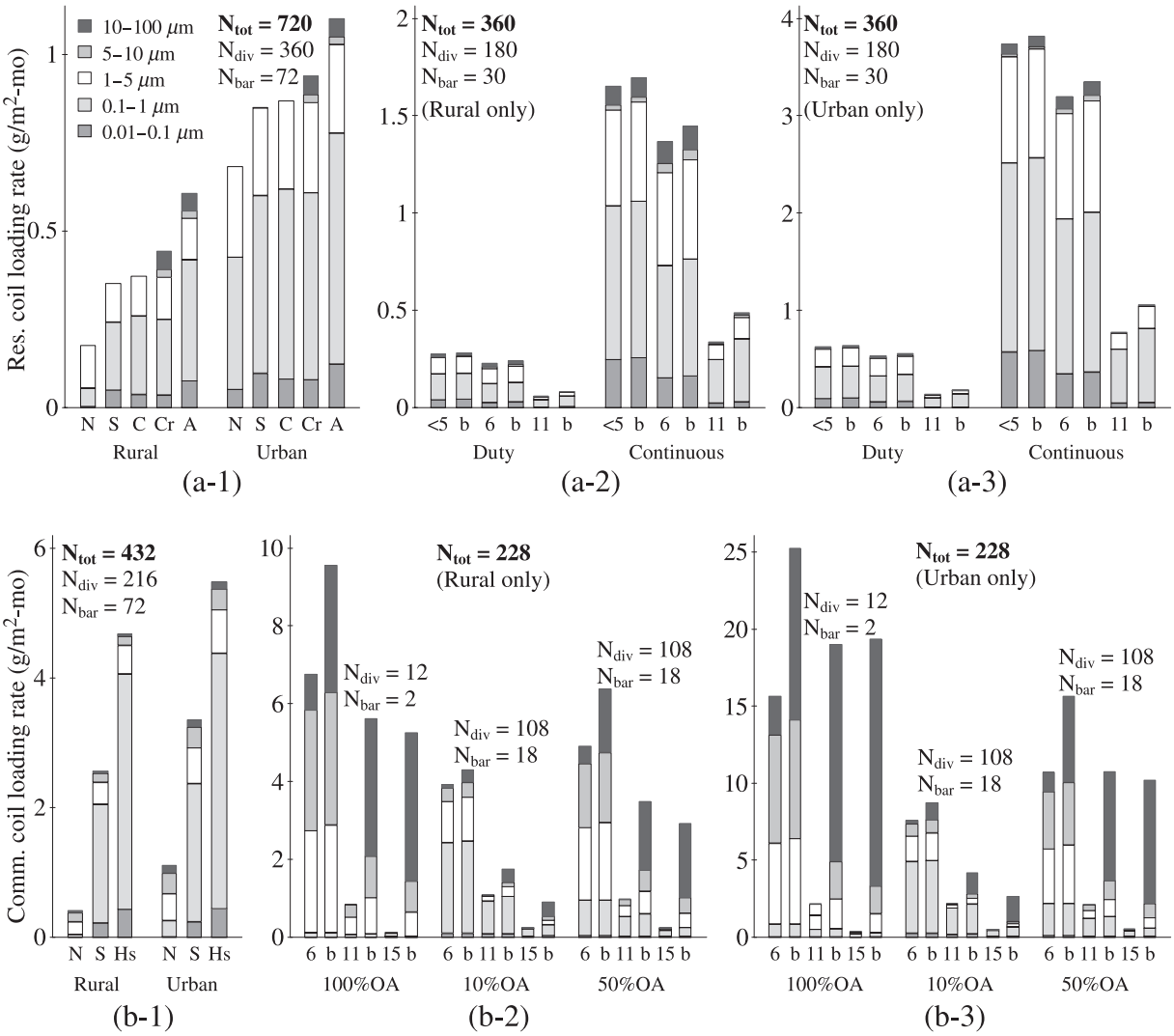

Fig. 5 Size-resolved (a) residential and (b) commercial coil loading rates (g/m^2 month), for (1) Emission parameters within each Ambient distribution, and Filtration parameters within each Flow case, for (2) Rural and (3) Urban distributions. Parameter codes on x-axes are listed in Table 3. N_{bar} represents number of scenarios used to make each bar, N_{div} for each division of plot, and N_{tot} for total plot (differences in values between each plot reflect elimination of non-unique scenarios)

to employ a time-averaged model. This assumption is reasonable for many buildings, but there are possible scenarios that would violate it. A further assumption is that this entire analysis considered only spherical particles despite the fact that some sources, such as combustion processes, produce agglomerated sub-micrometer particles. Additionally, this model assumed that floor loading and resulting resuspension emission rates are independent of the outdoor distribution and it considered resuspension as the only residential indoor source of large diameter particles. However, examinations of loaded HVAC components reveal that much of the loading can be attributed to larger, irregular particles (above 10 μm) and fibers with characteristic lengths of a millimeter or greater (Ahn and Lee, 2005; Siegel, 2002). These larger, irregular particles would likely have a greater relative effect on the increased pressure drop for the filters and the coils, because larger particles deposit at the leading edge of filters and coils (Siegel and Nazaroff, 2003), which has the largest effect on increasing pressure drop. Finally, the filter loading rates are likely the lower limits of loading because we neglected that filter efficiency typically increases with loading (Hanley et al., 1994).

Comparing these calculated loading rates with others found in the literature has proven to be difficult. We have only been able to locate anecdotal reports that confirm that filters and coils in real settings load over time (Ahn and Lee, 2005; Braun, 1986; Palani et al., 1992). There are other examples in the literature of filter, coil, and duct loading in laboratory settings that have similar findings (ARTI, 2004; Hanley et al., 1994; Krafthefer and Bonne, 1986; Krafthefer et al., 1987).

The IAQ implications of filter, coil, and duct loading are multifaceted. Loaded biologically active material can potentially colonize moist HVAC components

(Hugenholtz and Fuerst, 1992) and resuspend into the air stream (Batterman and Burge, 1995). Also, the higher removal efficiency of a loaded filter (Hanley et al., 1994) will lead to reduced particle concentrations in the space, but a loaded filter affects IAQ chemically as well. Ozone present in the air can heterogeneously react with the large surface area of the filter cake that accumulates on used filters, leading to ozone removal and the production of byproducts, such as formaldehyde (Hyttinen et al., 2003; Zhao et al., 2007) and ultrafine particles (Bekö et al., 2005). With more insight into the ozone/filter reaction process, the results here could be extended to the development of a deposition/diffusion/reaction model for HVAC filters.

As filters and coils load with time, the pressure drop across them increases (ARTI, 2004; Hanley et al., 1994; Siegel and Nazaroff, 2003). Figure 6 demonstrates how the relative pressure drop changes with normalized mass loaded for three of the filters (the information used to construct this plot was not available for the MERV <5 filter) and the dry, isothermal coil used in this study. For residential or other small-volume air systems with one-speed fans, the increased pressure drop can cause a reduction in flow, leading to a decrease in fan and compressor power draw, as well as decreased system heating or cooling efficiency and capacity (Parker et al., 1997). However, larger-volume air commercial systems typically have a variable-speed fan, so an increased pressure drop across a filter or a coil will lead to increased fan energy requirements (Fisk et al., 2002), as well as more cooling to remove the energy added to the air by the fan.

Coil fouling can also have energy consequences in the form of reduced heat transfer, because of the insulating layer of particle cake that forms on the heat exchanger surfaces. This effect is generally thought to be less important from an energy perspective than the increased pressure drop across the coil. For instance, Krafthefer et al. (1987) reported that, for a residential heat pump condenser coil, 87% of the loss of capacity and efficiency was because of the increased pressure drop. Additionally, most of the particles that deposit on a coil are on the leading edge of the heat exchanger (Siegel and Nazaroff, 2003) and little heat transfer actually occurs on these parts of the coil. However, one study reported that coil loading increased the heat transfer because of the additional turbulence from the increased surface area and roughness because of particle deposition (ARTI, 2004).

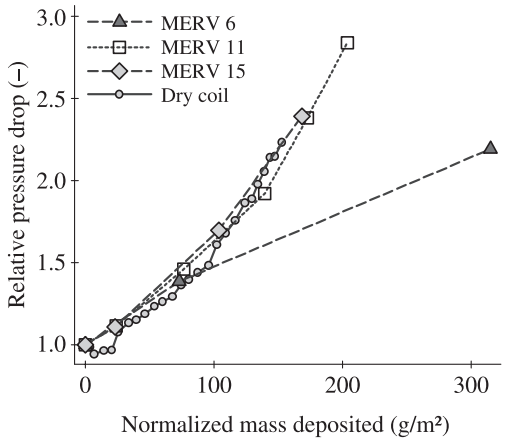

Fig. 6 Effect of normalized mass deposited (g/m^2) on relative pressure drop ($\Delta P/\Delta P_{initial}$) for MERV 6, 11, and 15 filters and Dry coil (Siegel, 2002) in this study

Buildings are responsible for approximately one-third of US energy use (EIA, 2002), and of that, about one-third is used for heating and cooling. Given these statistics, it becomes clear that even small decreases in heating or cooling capacity for HVAC systems can lead to substantial economic impacts, on a building and national scale. Accurately predicting (and maintaining) filter changing or coil cleaning can have a noticeable impact on energy demand and consumption (Montgomery and Baker, 2006). For the loading results herein, to estimate changing or cleaning schedules based on pressure drop increase, divide the mass deposited that correlates to a particular pressure drop increase (g/m^2) in Figure 6 by the loading rate (g/m^2 month) to get the time between changing or cleaning (in months). The curves presented in Figure 6 are reasonable starting points for estimating maintenance schedules; however, knowledge of how filter and coil loading affect pressure drop over time in real environments, rather than in laboratory settings, is preferable.

Conclusions

This paper presented the results of a comprehensive modeling effort to predict loading rates for residential and commercial HVAC filters, coils, and ducts, applying both experimental and modeled results for the input parameters. We report results for 720 unique residential parameter combinations modeled and between 444 and 648 unique commercial parameter combinations, depending on the particular HVAC component. The residential and commercial loading rates varied over a very large range, depending on the input parameters. For each set of unique parameter combinations, the medians for the predicted residential and commercial loading rates were 2.97 and 130 g/m^2 month for the filter loading rates, 0.756 and 4.35 g/m^2 month for the coil loading rates, 0.0051 and 1.00 g/month for the supply duct loading rates, and 0.262 g/month for the commercial return duct loading rates.

Based on the assumptions underlying the residential and commercial modeling, the following conclusions can be drawn from this work:

- Commercial buildings have larger loading rates than residential buildings, particularly for the filters.
- Residential loading rates are most influenced by the component itself as well as by the outdoor distribution, indoor sources, HVAC filters, and time of operation.
- Commercial loading rates are most influenced by the same parameters as residential systems, as well as by the fraction of ventilation vs. recirculation air.
- The influence of the coil and ducts on loading rates can be neglected for components other than themselves, for both residential and commercial buildings.
- The influence of indoor sources on loading rates decreases as the mass of the outdoor distribution increases, particularly for commercial buildings.
- The influence of different size ranges of particles on loading depends on whether the building is residential or commercial, because of the commercial ventilation air intake.
- For filters of different efficiencies, the actual contribution to filter loading is much more similar for particles over 1 μm than for particles smaller than 1 μm.
- Filter bypass has a larger relative effect on coil loading than on filter loading rates.

These results provide insight into IAQ and energy consequences that can result from particle deposition on HVAC components, and once validated, they can be used to estimate filter changing and coil cleaning schedules.

Acknowledgements

This research was funded by the National Science Foundation (IGERT Award DGE-0549428), the 3M Foundation (Non-tenured Faculty Award), and the American Society of Heating, Refrigerating and Air-Conditioning Engineers (New Investigator Award). The authors are grateful for careful reviews of the manuscript by Donghyun Rim and Atila Novoselac.

References

ACCA (1995) *Manual D: Residential Duct Systems*, Washington, DC, Air Conditioning Contractors of America.

Ahn, Y.C. and Lee, J.K. (2005) Characteristics of air-side particulate fouling materials in finned-tube heat exchangers of air conditioners, *Part. Sci. Technol.*, **23**, 297–307.

ARTI (2004) *The Role of Filtration in Maintaining Clean Heat Exchanger Coils*, Arlington, VA, Air-Conditioning and Refrigeration Technology Institute, ARTI-21CR/611-40050-01.

ASHRAE (2004) *Ventilation and Acceptable Indoor Air Quality in Low-Rise Residential Buildings*, Atlanta, GA, American Society of Heating, Refrigerating, and Air-Conditioning Engineers (ASHRAE Standard 62.2-2004).

ASHRAE (2007) *Method of Testing General Ventilation Air-Cleaning Devices for Removal Efficiency by Particle Size*, Atlanta, GA, American Society of Heating, Refrigerating, and Air-Conditioning Engineers (ASHRAE Standard 52.2-2007).

Batterman, S.A. and Burge, H. (1995) HVAC systems as emission sources affecting indoor air quality: a critical review, *HVAC&R Res.*, **1**, 61–80.

Bekö, G., Tamas, G., Halás, O., Clausen, G. and Weschler, C. (2005) Ultra-fine particles as indicators of the generation of oxidized products on the surface of used air filters. In: *Proceedings of Indoor Air* '05, Beijing, International Conference on Indoor Air Quality and Climate, Vol. 2, 1521–1525.

Bekö, G., Halás, O., Clausen, G. and Weschler, C.J. (2006) Initial studies of oxidation processes on filter surfaces and their impact on perceived air quality, *Indoor Air*, **16**, 56–64.

Braun, R.H. (1986) Problem and solution to plugging of a finned-tube cooling coil in an air handler, *ASHRAE Trans.*, **92**, 385–389.

EIA (2002) Energy Information Administration at the United States Department of Energy. http://www.eia.doe.gov/

Fisk, W.J., Faulkner, D., Palonen, J. and Seppanen, O. (2002) Performance and costs of particle air filtration technologies, *Indoor Air*, **12**, 223–234.

Hanley, J.T., Esnor, D.S., Smith, D.D. and Sparks, L.E. (1994) Fraction aerosol filtration efficiency of in-duct ventilation air cleaners, *Indoor Air*, **4**, 169–178.

Hinds, W.C. (1999) *Aerosol Technology: Properties, Behavior, and Measurement of Airborne Particles*, New York, Wiley.

Hugenholtz, P. and Fuerst, J.A. (1992) Heterotrophic bacteria in an air-handling system, *Appl. Environ. Microbiol.*, **58**, 3914–3920.

Hyttinen, M., Pasanen, P., Salo, J., Björkroth, M., Vartianen, M. and Kalliokoski, P. (2003) Reactions of ozone on ventilation filters, *Indoor Built Environ.*, **12**, 151–158.

Jaenicke, R. (1993) Tropospheric aerosols. In: Hobbs, P.V. (ed.) *Aerosol–Cloud–Climate Interactions*, San Diego, Academic Press, 1–31.

Klepeis, N.E., Apte, M.G., Gundel, L.A., Sextro, R.G. and Nazaroff, W.W. (2003) Determining size-specific emission factors for environmental tobacco smoke particles, *Aerosol Sci. Technol.*, **37**, 780–790.

Krafthefer, B. and Bonne, U. (1986) Energy use implications of methods to maintain heat exchanger coil cleanliness, *ASHRAE Trans.*, **92**, 420–431.

Krafthefer, B., Rask, D. and Bonne, U. (1987) Air-conditioning and heat pump operating cost savings by maintaining coil cleanliness, *ASHRAE Trans.*, **93**, 1458–1473.

Liu, D.L. and Nazaroff, W.W. (2001) Modeling pollutant penetration across building envelopes, *Atmos. Environ.* , **35**, 4451–4462.

Long, C.M., Suh, H.H., Catalano, P.J. and Koutrakis, P. (2001) Using time- and size-resolved particulate data to quantify indoor penetration and deposition behavior, *Environ. Sci. Technol.*, **35**, 2089–2099.

Montgomery, R.D. and Baker, R. (2006) Study verifies coil cleaning saves energy, *ASHRAE J.*, **48**, 34–36.

Nazaroff, W.W. and Klepeis, N.E. (2004) Environmental tobacco smoke particles. In: Morawska, L. and Salthammer, T. (eds) *Indoor Environment: Airborne Particles and Settled Dust*, Weinheim, Wiley VCH, 245–274.

Palani, M., O'Neal, D. and Haberl, J. (1992) The effect of reduced evaporator air flow on the performance of a residential central air conditioner, In: *Proceedings of the 1992 Symposium on Building Systems in Hot–Humid Climates*, Dallas, Texas, 20–26.

Parker, D.S., Sherwin, J.R., Raustad, R.A. and Shirey, D.B. III (1997) Impact of evaporator coil airflow in residential air-conditioning systems, *ASHRAE Trans.*, **103**, 395–405.

Riley, W.J., McKone, T.E., Lai, A.C.K. and Nazaroff, W.W. (2002) Indoor particulate matter of outdoor origin: importance of size-dependent removal mechanisms, *Environ. Sci. Technol.*, **36**, 200–207.

Seinfeld, J.H. and Pandis, S.N. (1998) *Atmospheric Chemistry and Physics*, New York, Wiley.

Siegel, J.A. (2002) *Particulate Fouling of HVAC Heat Exchangers*. PhD dissertation, Berkeley, University of California.

Siegel, J.A. and Nazaroff, W.W. (2003) Predicting particle deposition on HVAC heat exchangers, *Atmos. Environ.*, **37**, 5587–5596.

Siegel, J.A., McWilliams, J.A. and Walker, I.S. (2003) Comparison between predicted duct effectiveness from proposed ASHRAE standard 152P and measured field data for residential forced air cooling systems, *ASHRAE Trans.*, **109**, 503–512.

Sippola, M.R. and Nazaroff, W.W. (2003) Modeling particle loss in ventilation ducts, *Atmos. Environ.*, **37**, 5597–5609.

Sippola, M.R. and Nazaroff, W.W. (2004) Experiments measuring particle deposition from fully developed turbulent flow in ventilation ducts, *Aerosol Sci. Technol.*, **38**, 914–925.

Sippola, M.R. and Nazaroff, W.W. (2005) Particle deposition in ventilation ducts: connectors, bends and developing turbulent flow, *Aerosol Sci. Technol.*, **39**, 139–150.

Thatcher, T.L. and Layton, D.W. (1995) Deposition, resuspension, and penetration of particles within a residence, *Atmos. Environ.*, **29**, 1487–1497.

US Bureau of the Census (2005) *American Housing Survey*, Washington, DC.

Wallace, L.A. and Howard-Reed, C. (2002) Continuous monitoring of ultrafine, fine, and coarse particles in a residence for 18 months in 1999–2000, *J. Air Waste Manag. Assoc.*, **52**, 828–844.

Wallace, L.A., Emmerich, S.J. and Howard-Reed, C. (2004) Source strengths of ultrafine and fine particles due to cooking with a gas stove, *Environ. Sci. Technol.*, **38**, 2304–2311.

Ward, M. and Siegel, J.A. (2005) Modeling filter bypass: impact on filter efficiency, *ASHRAE Trans.*, **111**, 1091–1100.

Waring, M.S. and Siegel, J.A. (2007) An evaluation of the indoor air quality in bars before and after a smoking ban in Austin, Texas, *J. Exposure Sci. Environ. Epidemiol.*, **17**, 260–268.

Zhao, B. and Wu, J. (2006a) Modeling particle deposition from fully developed turbulent flow in ventilation duct, *Atmos. Environ.*, **40**, 457–466.

Zhao, B. and Wu, J. (2006b) Modeling particle deposition onto rough walls in ventilation duct, *Atmos. Environ.*, **40**, 6918–6927.

Zhao, P., Siegel, J.A. and Corsi, R.L. (2007) Ozone removal by HVAC filters, *Atmos. Environ.*, **41**, 3151–3160.